

南岭早侏罗世稀有金属成矿作用研究 ——以闽西南大坪花岗斑岩为例*

王锦荣^{1,2} 张哲坤^{3,4} 凌明星³ 吕新彪^{1**} 陈斌²

WANG JinRong^{1,2}, ZHANG ZheKun^{3,4}, LING MingXing³, LV XinBiao^{1**} and CHEN Bin²

1. 中国地质大学(武汉)资源学院, 武汉 430074

2. 中国冶金地质总局第二地质勘查院, 福州 350108

3. 同位素地球化学国家重点实验室, 中国科学院广州地球化学研究所, 广州 510640

4. 中国科学院大学, 北京 100049

1. Faculty of Earth Resources, China University of Geosciences, Wuhan 430074, China

2. The Second Geological Institute of China Metallurgical Geology Bureau, Fuzhou 350108, China

3. State Key Laboratory of Isotope Geochemistry, Guangzhou Institute of Geochemistry, Chinese Academy of Sciences, Guangzhou 510640, China

4. University of the Chinese Academy of Sciences, Beijing 100049, China

2019-04-25 收稿, 2019-09-20 改回.

Wang JR, Zhang ZK, Ling MX, Lv XB and Chen B. 2020. Early Jurassic rare metals mineralization in Nanling Region: A case of Daping granite porphyry in Southwest Fujian. *Acta Petrologica Sinica*, 36 (1): 125 – 140, doi:10.18654/1000-0569/2020.01.13

Abstract South China is an important region for rare metals' producing in China. Most of the deposits in this region are related to the high-evolution Li-F granites. The Daping granite porphyry is situated in the east edge of Nanling Range in Fujian Province. In this study, SIMS and LA-ICP-MS zircon U-Pb dating results yield ages of 186.7 ± 1.2 Ma and 190.7 ± 1.1 Ma for the Daping granite porphyry, which is the first report of Early Jurassic (200 ~ 180 Ma) magmatism and Nb-Ta mineralization in this area. Geochemically, they show metaluminous-peraluminous and display typical A-type granite characteristics, such as high SiO_2 (72.8% ~ 76.4%), K_2O and Zr + Nb + Ce + Y contents, high 10000Ga/Al, FeO^T/MgO ratios and low Zr, Hf, Ba, Sr, Ti and Eu contents. The granite underwent high degree of crystallization differentiation, and it is enriched in Nb_2O_5 and Ta_2O_5 , which achieved the industrial grades. In-situ zircon $\varepsilon_{\text{Hf}}(t)$ values range from -2.4 to 3.4, and their $\delta^{18}\text{O}$ range from 6.0‰ to 6.6‰. Based on regional geological data, it is proposed that the Daping granite porphyry is originated from the asthenosphere mantle, with 20% ~ 30% of crustal materials. During the evolution of the granites with enriched rare metals, the contents of F, Rb and Li in the melts increased with the increasing degree of their magmatic evolution. We chose a drill hole (ZK001) as the object of study to understand the enrichment processes of the Nb and Ta in this granite. As the depth of drill hole decreases, the ratios of Nb/Ta, Zr/Hf and Th/U goes down, while the ratio of Rb/Sr goes up, and the concentrations of Nb and Ta gradually increase. The rocks with high Nb and Ta concentrations normally contain high F contents (up to 0.8%), with high ratios of Y/Ho which also indicates that strong interactions occurred between the fluid and the magma. Late fluorine-rich fluids exsolving from the magmatic melts may play an important role in the concentration and fractionation of the Nb and Ta. In combination with the E-W trending Early Jurassic rock association (OIB-type gabbro and basalt, A-type granite) in the Nanling Range, the Daping granite and Fankeng bimodal volcanics are located along the east extension of the E-W trending rift belt of whom a great dispute has been put forward about its formation. Some people believe that this belt is a product of post-orogenic continental after the Triassic collision of Indochina block and the South China block; while others argue that the subduction of the paleo-Pacific plate played an important role in the formation of this belt. This event just occurred at the time and place in the transition from the Tethys tectonic domain to the paleo-Pacific tectonic domain. Through this study, we can deepen our understanding of regional

* 本文受国家重点研发计划 (2016YFC0600408、2017YFC0602301) 和中国地质调查局地质调查项目 (DD20160056) 联合资助。

第一作者简介: 王锦荣, 男, 1983 年生, 在职博士生, 矿物学、岩石学、矿床学专业, E-mail: zgbjrongw@163.com

** 通讯作者: 吕新彪, 男, 1962 年生, 教授, 博导, 主要从事矿床学、矿产普查与勘探研究, E-mail: lvxb_01@163.com

geological evolution and the formation of this rift belt and its volcanic rock assemblage.

Key words Daping granite porphyry; Nanling Range; Early Jurassic; Intra-continental extension; Zircon Hf-O isotope

摘要 华南地区是我国重要的稀有金属矿产区,绝大部分具经济规模的稀有金属矿床均与高演化的富 Li-F 花岗岩有成因联系。大坪花岗斑岩位于南岭构造带最东缘福建省永定地区,与区内 Nb-Ta 矿床形成有关。该岩体 SIMS 和 LA-ICP-MS 锆石 U-Pb 定年结果分别为 186.7 ± 1.2 Ma 和 190.7 ± 1.1 Ma,是华南少见的早侏罗世(200~180Ma)侵入的花岗岩侵入体,也是华南最早报道的早侏罗世稀有金属成矿事件。大坪花岗斑岩具高钾低镁、准铝质到弱过铝质的特征,属于高钾钙碱性花岗岩,并显示 A 型花岗岩的地球化学特征,如富硅(72.81%~76.44%)、高 $10000 \times \text{Ga}/\text{Al}$ 比值、高 $\text{FeO}^{\text{T}}/\text{MgO}$ 和高 Zr + Nb + Ce + Y 含量、亏损高场强元素和 Eu 负异常明显等。全岩体系低的 Zr/Hf、Nb/Ta 比值,指示岩浆具有较高的分异演化程度, Nb_2O_5 和 Ta_2O_5 均含量达到了花岗岩型稀有金属矿床的工业品位。花岗斑岩中锆石 Hf-O 同位素分析结果显示,其具有比较亏损的 Hf 同位素与比较均一的 O 同位素组成($\varepsilon_{\text{Hf}}(t) = -2.4 \sim 3.4$, $\delta^{18}\text{O} = 6.0\text{‰} \sim 6.6\text{‰}$)。结合微量元素地球化学特征,大坪花岗斑岩源区主要来源于软流圈地幔,并有约 20%~30% 壳源岩浆的加入,在成岩过程中发生了显著的分异结晶。晚期富氟的流体出熔并向上迁移可能对于 Nb 和 Ta 的再次富集与分异具有重要作用。大坪花岗斑岩与闽西南地区同时期的火山岩,如潘坑组双峰式火山岩,在空间上可与前人提出的“南岭山脉早侏罗世发育的东西向裂谷岩浆岩带(OIB 型玄武岩、辉长岩和 A 型花岗岩组合)”相对应,是该裂谷带向东的延伸。

关键词 大坪花岗斑岩;南岭;早侏罗世;板内伸展;锆石 Hf-O 同位素

中图分类号 P588.13; P597.3; P618.6

华南位于欧亚大陆的东南缘,是由多个块体或地体拼合增生而成的大陆板块,主要构造单元包括扬子地块、江南造山带、华夏地块等。华南经历了多期构造运动,发育了多期次构造-岩浆活动,其中以中生代的构造-岩浆活动最为强烈,整体出露大约 $220,000\text{km}^2$ 的火山岩和侵入岩(Zhou *et al.*, 2006; Wang *et al.*, 2011; Li *et al.*, 2012a; Sun *et al.*, 2012),其中大部分是燕山早期(中晚侏罗世)花岗岩(图 1a),与稀有金属矿产(W-Sn-Nb-Ta)有非常密切的关系,是中国花岗岩与成矿作用研究的摇篮。

基于已经发表的的同位素数据统计(Zhou *et al.*, 2006),传统观点认为早侏罗世(200~180Ma)存在一个岩浆间歇期(图 1a)。但是随着分析技术的进步,华南各类火成岩石又积累相当数量的高质量数据资料,发现在早侏罗世南岭地区存在一条 E-W 向的岩浆带(图 1a),东起福建永定地区,经江西寻乌、龙南、定南地区,广东始兴、梅州,湖南宜章、道县、宁远地区,全长 500km 和宽 250km。以双峰式火山岩(OIB 型玄武岩和流纹岩)和 A 型花岗岩、碱性正长岩、橄榄辉长岩、角闪辉长岩为主要组合特征(Li *et al.*, 2003; 李献华等,2007),还伴随少量 S 型和 I 型花岗岩。这与前人认为在闽西-赣南-粤东地区发育一条侏罗世 E-W 向陆内伸展带(裂谷盆地群)是吻合的(舒良树等,2004)。关于南岭早侏罗世岩浆活动,虽然前人对其中的花岗岩(寨背、陂头、柯树北)及镁铁质岩石开展了部分研究,但是,关于其岩石成因及构造背景一直以来有着广泛的争议。例如,有学者认为这些花岗岩形成于印支运动的后造山伸展背景或者陆内伸展背景下(陈培荣等,2002;付建明等,2004;Chen *et al.*, 2008);有的学者则认为它们的形成与古太平洋板块俯冲引发的弧后拉张背景有关(谢昕等,2005; Zhou *et al.*, 2006; Jiang *et al.*, 2009a, b; 余心起等,2009; He *et al.*, 2010; Wang *et al.*, 2011; Sun *et al.*, 2012),也有学者认为这些花岗岩受从

晚三叠世开始的古太平洋板块俯冲影响,与板片断离或板片破坏引起软流圈地幔物质的上涌有关(Li and Li, 2007; Zhu *et al.*, 2010)。以上争议的关键在于目前仍无确切的资料来限定古特提斯构造域向古太平洋构造域转换的时代与空间位置。南岭构造带处于古特提斯构造域与古太平洋构造域的复合部位,是限定古特提斯构造域向古太平洋构造域转换时空的理想地区。

闽西南永定盆地位于南岭构造带的最东缘,区内出露大量的早侏罗世双峰式火山岩与侵入花岗斑岩,大坪岩体是近年来发现的一个具铌钽矿化的花岗斑岩体,铌钽含量达到花岗岩型铌钽矿床的最低工业品位,但其研究程度几乎空白,笔者挑选该岩体两个钻孔的新鲜样品进行系统的岩相学、锆石 U-Pb 年代学和原位 Hf-O 同位素分析,以查明其岩石成因及其动力学机制,这对制约该区两大构造域转换的时空关系具有重要意义。

1 地质背景

南岭构造带呈东西向展布,其西侧以萍乡-桂林断裂与扬子新元古代造山带相接,东侧以政和-大埔断裂与东南沿海晚中生代火山-侵入杂岩带接触,北侧以茶陵-广昌隐伏断裂和武夷山褶皱带相连,南界为博白-岑溪断裂(舒良树, 2006)。该构造带发育在华南前震旦纪-早古生代褶皱基底之上(舒良树等,2004;舒良树,2012),经历了早古生代末期、早中生代初期和晚中生代等多期构造-岩浆活动(Li *et al.*, 2004;舒良树等,2004)。区内晚中生代的构造岩浆活动与稀有金属(W-Sn-Nb-Ta)伴生关系密切(Mao *et al.*, 2013; Chen *et al.*, 2016; Zhang *et al.*, 2017b),广受大家关注。南岭构造带是研究华南东部从古特提斯构造域向古太平洋构造域

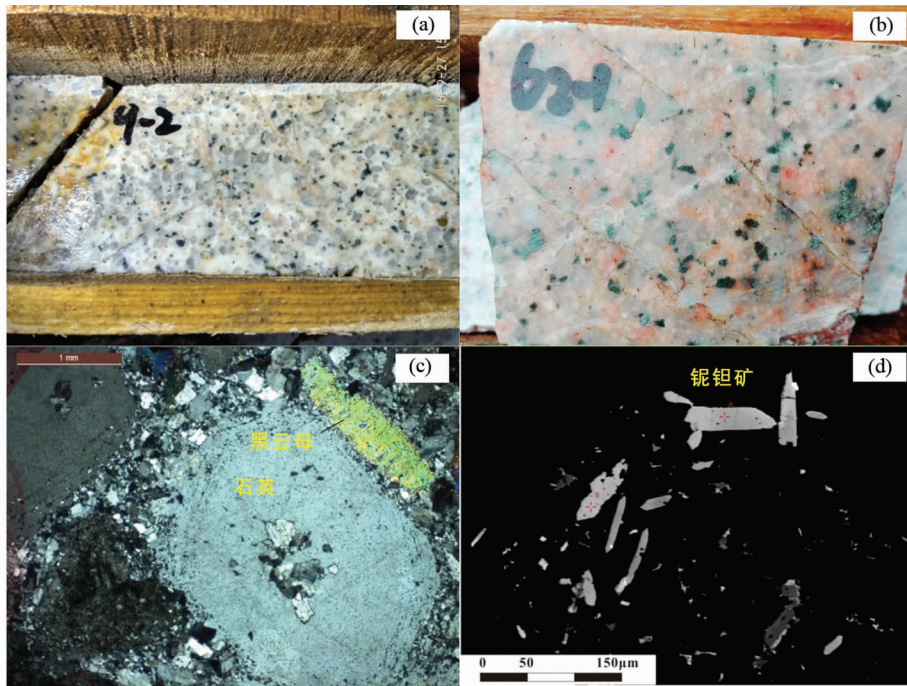


图2 福建大坪花岗斑岩手标本(a,b)和显微镜下钾长石和石英照片(c)及板状铌钽铁矿电子探针背散射图像(d)

Fig.2 Photos of specimens from the Daping granite porphyry (a, b), microphotograph of phenocrysts of quartz and feldspar (c) and backscattered image of columbite-tantalite (d)

对样品靶的锆石进行显微镜下透射光和反射光的观察和照相,以及阴极发光(CL)图像分析。制靶在中国科学院广州地球化学研究所同位素地球化学国家重点实验离子探针中心完成,CL图像分析在同位素国家重点实验电子探针微区分析实验室 Gatan Mono CL3 型阴极发光系统上完成。锆石 SIMS 原位 U-Pb 定年参数条件为,一次离子流为强度约 8Na、束斑大小为 $20 \times 30 \mu\text{m}$ 。 $\delta^{18}\text{O}$ 分析条件为,一次离子流为强度约 2nA、束斑大小为 $10 \mu\text{m}$,实验采用 91500 和清湖锆石作为标样。SIMS 锆石 U-Pb 定年和 $\delta^{18}\text{O}$ 分析均在同位素地球化学国家重点实验离子探针中心 Cameca IMS 1280HR 上完成,详细过程参考 Li *et al.* (2009)。部分样品锆石原位 U-Pb 定年在中国科学院广州地球化学研究所中国科学院矿物与成矿学重点实验室完成,剥蚀束斑 $29 \mu\text{m}$,频率 8Hz,所用仪器为激光剥蚀等离子质谱(LA-ICP-MS),其中剥蚀系统为 Resolution S-155,剥蚀系统为 Agilent 7900 ICP-MS,详细过程参考 Li *et al.* (2012a) and Liu *et al.* (2016)。锆石原位 Lu-Hf 同位素分析在武汉上谱分析科技有限公司完成,剥蚀束斑 $44 \mu\text{m}$,频率 8Hz,所用仪器为相干 193nm 准分子激光剥蚀系统(GeoLasPro HD)和多接收质谱 MC-ICP-MS (Neptune Plus)。实验采用 91500 和 GJ-1 作为标样,91500 的 $^{176}\text{Hf}/^{177}\text{Hf}$ 比值为 0.282310 ± 25 。 ε_{Hf} 计算采用的 ^{176}Lu 的衰变常数为 1.867×10^{-11} (Scherer *et al.*, 2001),球粒陨石 $^{176}\text{Hf}/^{177}\text{Hf} = 0.282793$, $^{176}\text{Lu}/^{177}\text{Hf} = 0.0332$ (Blichert-Toft and Albarède, 1997)。亏损地幔 Hf 模式年龄(t_{DM})采用 $^{176}\text{Hf}/^{177}\text{Hf} = 0.283251$, $^{176}\text{Lu}/^{177}\text{Hf} = 0.0384$ 计算 (Vervoort and

Blichert-Toft, 1999),二阶段 Hf 模式年龄($t_{\text{DM2}}^{\text{c}}$)采用平均大陆壳 $^{176}\text{Lu}/^{177}\text{Hf} = 0.015$ 计算 (Griffin *et al.*, 2004)。

全岩粉末样品选择新鲜岩石样品用无污染颚式破碎机及玛瑙碾钵破碎至 200 目以下。全岩的主微量分析测试在中国科学院广州地球化学研究所同位素地球化学国家重点实验室完成。主量分析称取适量样品干燥后,放入马弗炉内进行 900 度灼烧以测其烧矢量,称取烧失后的样品,按 1:8 的比例用纯四硼酸锂稀释后用 1250℃ 的温度熔成玻璃,然后在 Rigaku ZSX 100e X 射线荧光光谱仪进行主量元素的分析,分析的精度优于 1%。将样品烘干后的 200 目样品放入洗净的杯子中,加入 4N 高纯硝酸 3mL,在 190℃ 的烘箱内加热 4~6 个小时,蒸干后用 100mL 4N 硝酸加热提取,加 5mL milli-Q 水摇匀后,用 PE Elan 6000 型 ICP-MS 分析微量元素组成。

3 分析结果

3.1 锆石 U-Pb 定年

我们选择 Zk001 中 ZL-4(230m)、ZL-10(485m)和 ZL-11(595m)三个样品进行锆石 U-Pb 定年,其中 ZL-4 和 ZL-10 采用 SIMS 分析,ZL-11 采用 LA-ICP-MS 分析(表 1)。由于样品 ZL-4(230m)采样更浅,分异程度更高,与流体强烈相互作用,大部分锆石的晶格破坏,发生退晶化,没有获得很好的年龄数据,这里不做讨论。ZL-10(485m)和 ZL-11(595m)分异

表1 大坪花岗斑岩 LA-ICP-MS 和 SIMS 锆石 U-Pb 定年结果

Table 1 LA-ICP-MS and SIMS zircons U-Pb dating results for the Daping granite porphyry

测点号	Th U		Th/U	²⁰⁷ Pb/ ²³⁵ U		²⁰⁶ Pb/ ²³⁸ U		²⁰⁷ Pb/ ²³⁵ U		²⁰⁶ Pb/ ²³⁸ U	
	(×10 ⁻⁶)			Ratio	1σ	Ratio	1σ	Age (Ma)	1σ	Age (Ma)	1σ
ZL-10											
1	1347	1008	0.81	0.19973	1.91102	0.02929	1.51020	185	3	186	3
2	1058	758	0.77	0.19880	1.62715	0.02912	1.50035	184	3	185	3
3	2207	1962	0.87	0.20421	1.77026	0.02974	1.50560	189	3	189	3
4	2226	2005	0.84	0.20516	2.58452	0.02974	1.50691	189	4	189	3
5	821	555	0.72	0.19984	1.77483	0.02930	1.53770	185	3	186	3
6	907	492	0.64	0.19259	2.68684	0.02849	1.50390	179	4	181	3
7	1152	866	0.64	0.20304	1.62825	0.02928	1.51282	188	3	186	3
8	989	731	0.80	0.20163	1.83238	0.02961	1.50003	187	3	188	3
9	1565	1312	0.94	0.20236	1.76906	0.02979	1.50274	187	3	189	3
10	811	647	0.75	0.20196	1.66504	0.02935	1.50078	187	3	186	3
11	988	742	0.72	0.20319	1.97462	0.02956	1.73927	188	3	188	3
12	943	701	0.73	0.20160	1.63646	0.02943	1.50840	186	3	187	3
13	1001	731	0.75	0.19967	1.65563	0.02918	1.50799	185	3	185	3
14	2411	2411	1.01	0.20510	1.59362	0.02994	1.50577	189	3	190	3
15	1038	787	0.76	0.19967	1.75022	0.02919	1.51830	185	3	185	3
16	1176	912	0.74	0.20203	1.64236	0.02937	1.50915	187	3	187	3
ZL-11											
1	1560	2893	0.54	0.21552	0.00497	0.03079	0.00045	198	4	196	3
2	565	1048	0.54	0.21347	0.00614	0.03054	0.00039	196	5	194	2
3	4407	2886	1.53	0.20791	0.00420	0.03045	0.00035	192	4	193	2
4	2423	7530	0.32	0.20838	0.00394	0.03005	0.00037	192	3	191	2
5	254	349	0.73	0.19591	0.01144	0.02986	0.00059	182	7	190	4
6	1795	3537	0.51	0.20164	0.00398	0.02898	0.00032	187	3	184	2
7	1529	5122	0.30	0.20553	0.00375	0.02958	0.00031	190	3	188	2
8	885	2695	0.33	0.21027	0.00718	0.02985	0.00063	194	6	190	4
9	624	3339	0.19	0.20907	0.00499	0.02970	0.00041	193	4	189	3
10	435	496	0.88	0.21626	0.00810	0.02953	0.00040	199	7	188	3
11	2209	4269	0.52	0.20359	0.00356	0.02935	0.00027	188	3	186	2
12	1910	1589	1.20	0.20685	0.00455	0.03050	0.00035	191	4	194	2
13	1056	2874	0.37	0.21651	0.00538	0.03048	0.00046	199	4	194	3
14	149	347	0.43	0.19162	0.00948	0.02973	0.00050	178	8	189	3
15	3275	3460	0.95	0.21554	0.00534	0.03047	0.00043	198	4	193	3
16	445	859	0.52	0.21293	0.00591	0.03011	0.00041	196	5	191	3
17	319	544	0.59	0.20467	0.01101	0.03063	0.00062	189	9	194	4
18	4280	4371	0.98	0.21903	0.00391	0.03018	0.00038	201	3	192	2
19	797	913	0.87	0.20212	0.00508	0.02950	0.00037	187	4	187	2
20	3100	6511	0.48	0.21195	0.00480	0.03024	0.00050	195	4	192	3
21	140	401	0.35	0.19642	0.00942	0.03026	0.00055	182	8	192	3
22	631	1508	0.42	0.20872	0.00522	0.03035	0.00039	192	4	193	2

程度相对较低,样品有许多锆石保留了结晶的形貌,没有发生退晶化(图3),可以获得很好的谐和年龄和加权平均年龄。

样品 ZL-10(485m),锆石多呈自形板状,选择无色透明没有包裹体和裂隙的锆石进行 SIMS 微区分析,17 个分析点的 Th/U 比值变化于 0.54 ~ 1 之间,且绝大多数 > 0.6,其形态和 CL 图像显示出明显的振荡环带,都表明它们为典型的岩浆成因锆石。15 颗锆石的 ²⁰⁶Pb/²³⁸U 年龄变化于 185 ~

190Ma,普通铅含量很低,其中 2 颗锆石的 ²⁰⁶Pb/²³⁸U 年龄偏小为 181Ma,分析误差偏大。17 颗锆石的 ²⁰⁶Pb/²³⁸U 与 ²⁰⁷Pb/²³⁵U 谐和年龄为 186.7 ± 1.2Ma (MSWD = 1.5),17 颗锆石 ²⁰⁶Pb/²³⁸U 加权平均年龄为 186.6 ± 0.8Ma (MSWD = 0.97,图 3a)。样品 ZL-11 (595m),锆石形貌类似于 ZL-10 (485m),且它们的 Th/U 比值集中于 0.3 ~ 1.0,绝大部分为典型的岩浆锆石特征,少数几颗可能为热液锆石。所测的 22 颗锆石的 ²⁰⁶Pb/²³⁸U 年龄变化于 184 ~ 196Ma,它们的加权平

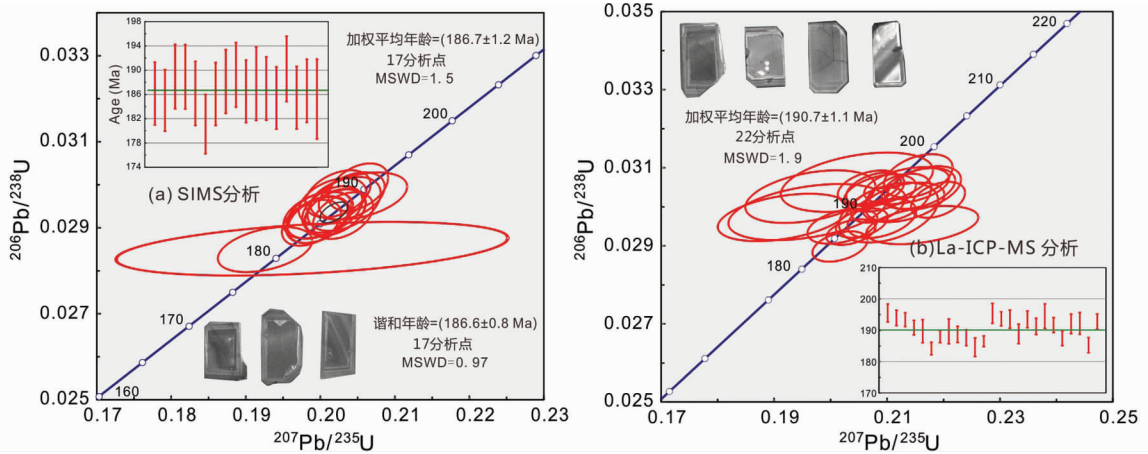


图3 大坪花岗斑岩的锆石形貌和谐和年龄及加权平均年龄

Fig.3 Zircon U-Pb concordian diagram, weighted average ages and morphology for the Daping granite porphyry

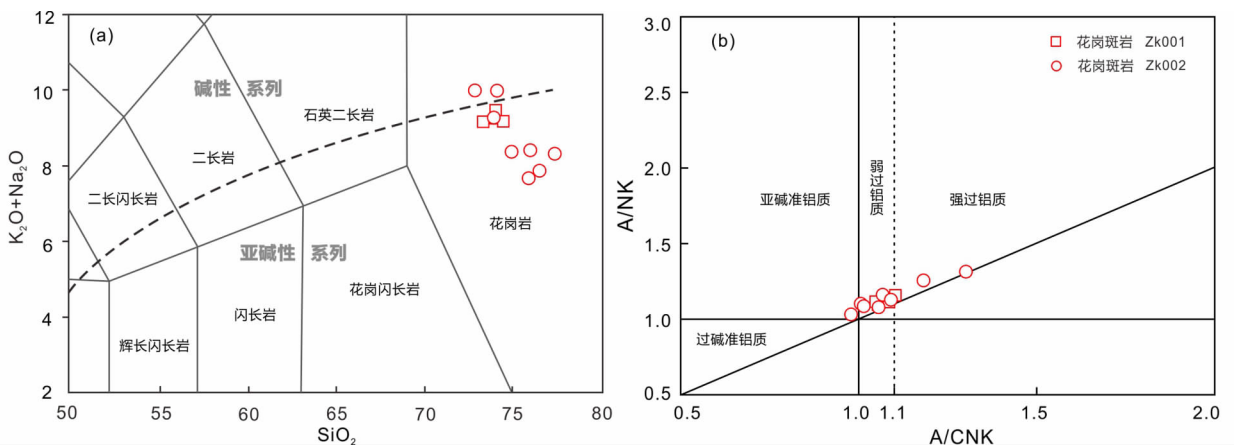


图4 大坪花岗斑岩($K_2O + Na_2O$)- SiO_2 (a, 据 Peccerillo and Taylor, 1976) 和 A/NK - A/CNK (b, 据 Maniar and Piccoli, 1989) 图解

Fig.4 Diagrams of ($K_2O + SiO_2$) vs. SiO_2 (a, after Peccerillo and Taylor, 1976) and A/NK vs. A/CNK (b, after Maniar and Piccoli, 1989)

均年龄为 190.7 ± 1.1 Ma (MSWD = 1.9, 图 3b)。综上, 大坪花岗斑岩的形成时代为 187 ~ 191 Ma, 与藩坑组火山岩活动时代近似, 为早侏罗世岩浆活动产物。

3.2 岩石地球化学特征

岩石地球化学分析显示大坪花岗斑岩的主量元素含量变化不是很大, 但是随着空间变化显示一定的趋势(表 2)。总体特征为: 硅较高 ($SiO_2 = 72.81\% \sim 77.30\%$)、偏碱(全碱 $ALK(Na_2O + K_2O) = 7.70\% \sim 10.03\%$)、富钾 ($K_2O = 4.11\% \sim 5.87\%$)、碱铝指数 (AKI 值) 变化于 0.55 ~ 0.73。在 ($K_2O + Na_2O$)- SiO_2 图中落在亚碱性花岗岩系列区域, 在 A/NK - A/CNK 图解上大部分落在弱过铝质范围(图 4)。这与同时期内陆 200 ~ 170 Ma 呈 E-W 向展布的典型 A 型花岗岩, 如赣南陂头岩体、寨背岩体和温公花岗岩 (Zhu *et al.*,

2010; 甘成势等, 2016; Gan *et al.*, 2017) 特征类似。此外, 主要元素的 Harker 图解(图 5)上, 大坪花岗斑岩普遍低 $Fe_2O_3^T$ (0.87% ~ 2.4%)、 MnO (0.04% ~ 0.24%)、 MgO (0.17% ~ 0.20%)、 CaO (0.09% ~ 0.62%)、 TiO_2 (0.01% ~ 0.03%) 和 P_2O_5 (0.01% ~ 0.04%)。

稀土元素配分曲线和微量元素蛛网图解如图 6。大坪岩体的 ΣREE 为 $56.2 \times 10^{-6} \sim 218 \times 10^{-6}$, $(La/Yb)_N = 0.80 \sim 2.15$, 表明岩体轻重稀土元素分异不明显。 $\delta Eu = 0.04 \sim 0.29$, 具有明显的 Eu 负异常, $\delta Ce = 0.75 \sim 1.27$, 无明显 Ce 异常, 显示有明显的 M 型四分组效应(图 6a)。大坪岩体微量元素蛛网图整体呈现右倾的趋势, 其中高场强元素 Th、U、Ta、Nb、Hf 等相对富集, 大离子亲石元素 Ba、Sr 等相对亏损, Rb 元素相对富集, 有明显的 Ti 亏损(图 6b)。岩体有着高的 Rb/Sr 比值(24.5 ~ 140.2) 和 Y/Ho 比值(19.5 ~ 36.7), 低的 Zr/Hf 比值(4.1 ~ 11) 和 Nb/Ta 比值(0.86 ~ 3.78)。

表2 大坪花岗斑岩的主量元素 (wt%) 和微量元素 ($\times 10^{-6}$) 成分Table 2 Major (wt%) and trace ($\times 10^{-6}$) element compositions of the Daping granite porphyry

位置 样品号 标高 (m)	ZK1002						ZK1001					
	ZL-3	ZL-4	ZL-5	ZL-6	ZL-7	ZL-8	ZL-9	DP-0	DP-43	DP-178	DP-319	DP-461
	155	230	330	380	380	430	545	0	43	178	319	461
SiO ₂	73.96	73.98	74.41	73.28	77.30	75.92	75.83	74.87	72.81	74.06	73.87	76.44
Al ₂ O ₃	14.93	14.70	14.09	14.52	12.25	12.32	14.06	14.82	15.38	13.71	14.73	12.27
Fe ₂ O ₃ ^T	1.00	0.87	0.86	1.46	0.87	1.36	0.88	0.76	0.98	2.49	0.91	1.77
CaO	0.31	0.19	0.34	0.38	0.47	0.62	0.42	0.09	0.21	0.45	0.29	0.54
MgO	0.07	0.07	0.10	0.11	0.07	0.07	0.07	0.19	0.07	0.16	0.08	0.07
K ₂ O	4.12	4.26	4.19	4.17	4.47	4.90	2.74	4.6	4.11	5.87	4.11	4.4
Na ₂ O	5.16	5.25	5.02	5.03	3.88	3.54	4.96	3.8	5.92	4.15	5.2	3.5
TiO ₂	0.03	0.02	0.02	0.02	0.03	0.04	0.03	0.01	0.01	0.01	0.01	0.03
MnO	0.037	0.041	0.057	0.046	0.041	0.07	0.04	0.04	0.08	0.17	0.06	0.24
P ₂ O ₅	0.04	0.04	0.04	0.03	0.03	0.04	0.03	0.01	0.01	0.01	0.01	0.02
LOI	0.44	0.33	0.39	0.51	0.53	0.57	0.81	1.06	0.25	1.88	0.31	0.79
Total	100.0	99.7	99.5	99.6	99.9	99.4	99.9	100.3	99.8	103.0	99.6	100.1
A/NK	1.15	1.11	1.10	1.14	1.09	1.11	1.26	1.32	1.08	1.04	1.13	1.17
A/CNK	1.10	1.08	1.05	1.08	1.01	1.01	1.18	1.30	1.06	0.98	1.09	1.07
Rb	1200	1100	933	1050	619	600	539	580	837	854	595	408
Sr	11.5	9.4	26.1	8.81	14.9	24.5	17.2	9.9	5.97	8.26	12.3	15.3
Ba	18	24.6	34.5	16.6	42.7	94.5	20.9	63.1	8.46	65.6	24	26.2
Th	25	17	27.2	14.3	34.1	38.5	28.8	38.7	21.3	19.4	15.5	46.5
U	13.7	14.6	14.4	10.3	13.7	12.9	12.5	4.95	8.96	19.9	8.53	12.6
Nb	111	115	130	103	149	173	144	114	84.1	116	89.8	108
Ta	125	125	125	68.1	55.8	58.7	38.1	83.3	97.5	106	70.9	41.4
Zr	48.3	41.3	53	52.4	90.7	96.6	107	55.1	43.5	58.1	55.5	107
Hf	9.18	7.12	9.68	8.03	10.2	8.85	11	10.7	10.7	11.4	10.5	12.6
Li	172	110	6.8	42.8	5.06	5.02	35.6	13.2	388	23.9	73.4	19.6
Cs	3.1	3.77	1.79	4.46	1.76	1.18	3.16	1.99	4.95	5.45	2.83	2.2
Be	8.15	5.56	4.84	5.69	5.07	20.1	12.3	4.66	8.13	3.07	4.44	128
Ga	52.7	46.3	44	55.2	37.6	35.3	41.8	51.3	53.2	49.5	38.7	35.8
Y	9.17	7.1	7.27	10.7	24.6	56	32.1	17.3	7.21	10.6	8.43	64.2
La	9.92	15.7	8.48	9.55	28.7	35.8	22.6	9.65	10.4	10.2	14.9	34.1
Ce	27.2	42.7	24.9	26	74.2	86.7	56.6	15.9	27.3	29.3	34.2	93
Pr	3.07	4.42	2.64	2.86	7.96	9.72	6.22	2.71	3.08	3.06	3.56	10.8
Nd	6.3	8.72	5.4	5.81	17	23.4	14.7	7.4	6.88	7.48	8.15	30.4
Sm	1.27	1.56	1.04	1.19	3.14	4.76	2.93	1.69	1.17	1.4	1.37	5.93
Eu	0.033	0.035	0.015	0.015	0.031	0.072	0.040	0.160	0.040	0.030	0.030	0.070
Gd	1.05	1.25	0.87	1	2.55	4.13	2.49	1.62	0.62	0.74	0.71	3.89
Tb	0.24	0.21	0.19	0.24	0.49	0.92	0.51	0.37	0.17	0.23	0.23	1.01
Dy	1.84	1.43	1.42	1.85	3.52	6.56	3.48	2.99	1.48	2.13	1.7	8.06
Ho	0.47	0.35	0.36	0.48	0.9	1.66	0.88	0.67	0.35	0.49	0.37	1.89
Er	2.05	1.51	1.64	2.1	3.79	6.75	3.55	2.79	1.51	2.12	1.79	7.79
Tm	0.67	0.47	0.54	0.68	1.13	1.81	1	0.75	0.42	0.61	0.5	1.87
Yb	6.18	4.27	5.14	6.3	10	15.1	8.82	8.16	4.68	6.34	4.97	17.3
Lu	1.13	0.77	0.95	1.16	1.83	2.71	1.6	1.32	0.74	0.97	0.8	2.72
∑REE	61.4	83.4	53.6	59.2	155.2	200.1	125.4	56.2	58.8	65.1	73.3	218.8
Rb/Sr	87.0	106.4	35.7	113.5	41.5	24.5	31.3	58.6	140.2	103.4	48.4	26.7
Ga/Al	6.67	5.95	5.90	7.18	5.80	5.41	5.62	6.54	6.53	6.82	4.96	5.51
Zr/Hf	5.26	5.80	5.48	6.53	8.89	10.92	9.73	5.15	4.07	5.10	5.29	8.49
Nb/Ta	0.89	0.92	1.04	1.51	2.67	2.95	3.78	1.37	0.86	1.09	1.27	2.61
Th/U	1.82	1.16	1.89	1.39	2.49	2.98	2.30	7.82	2.38	0.97	1.82	3.69
Y/Ho	19.51	20.29	20.19	22.29	27.33	33.73	36.48	25.82	20.60	21.63	22.78	33.97
Zr + Nb + Ce + Y	195.7	206.1	215.2	192.1	338.5	412.3	339.7	202.3	162.1	214	187.9	372.2
Y + Nb	120.17	122.1	137.27	113.7	173.6	229	176.1	131.3	91.31	126.6	98.23	172.2
T _{zr} (°C)	696	683	699	694	742	745	767	720	683	699	705	759

注:其中 DP-0 ~ 461 引自刘永超等(2017)

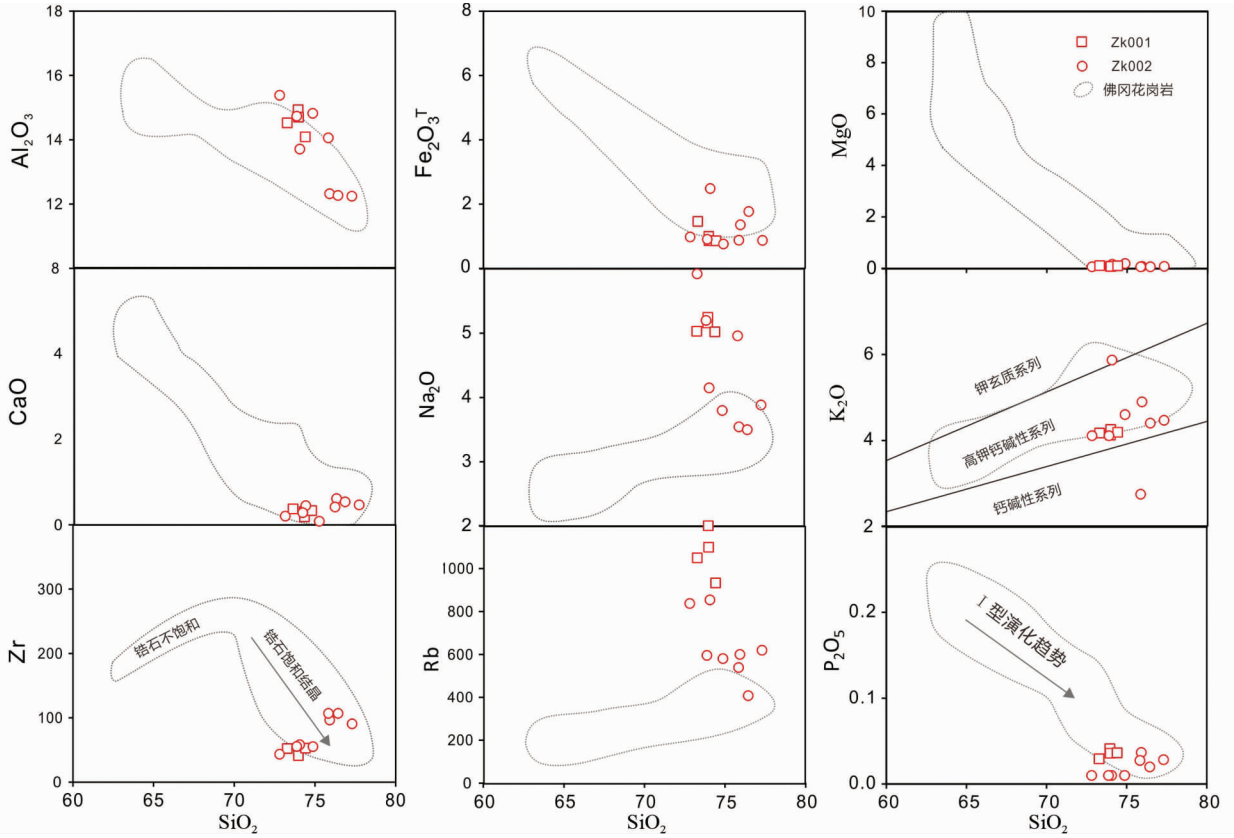


图5 大坪花岗斑岩主要元素的 Harker 图解

佛冈岩体数据引自 Li *et al.* (2007)

Fig.5 Harker diagrams for the Daping granite porphyry

The data of Fogang granite is after Li *et al.* (2007)

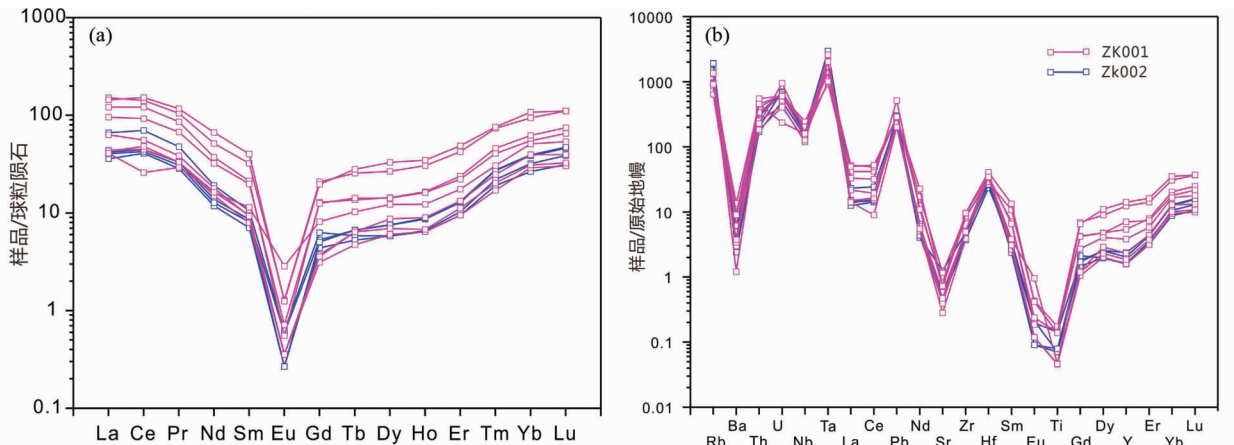


图6 大坪花岗斑岩球粒陨石标准化稀土元素图解(a)和原始地幔标准化微量元素蛛网图(b) (标准化值据 McDonough and Sun, 1995)

Fig.6 Chondrite-normalized REE pattern diagram (a) and primitive mantle-normalized trace element diagram (b) for the Daping granite porphyry (normalization values after McDonough and Sun, 1995)

3.3 锆石 Hf-O 同位素分析

对其中 SIMS 定年样品 ZL-10(485m)的锆石颗粒分别进

行了原位 Hf-O 同位素测定,详细分析结果列于表3。17 颗锆石的 Hf 同位素变化比较大,均显示了比较亏损的源区特征, $^{176}\text{Hf}/^{177}\text{Hf}=0.282617 \sim 0.282781$, 对应样品的 $\epsilon_{\text{Hf}}(t) =$

表3 大坪花岗斑岩锆石的 Hf-O 同位素组成

Table 3 Zircon Hf-O isotopic compositions from the Daping granite porphyry

测点号	$(^{176}\text{Yb}/^{177}\text{Hf})_s$	1σ	$(^{176}\text{Lu}/^{177}\text{Hf})_s$	1σ	$(^{176}\text{Hf}/^{177}\text{Hf})_s$	1σ	$\varepsilon_{\text{Hf}}(t)$	$t_{\text{DM2}}(\text{Ma})$	$\delta^{18}\text{O}$	2se
$t = 190\text{Ma}$										
1	0.110638	0.001910	0.003042	0.000048	0.282646	0.000009	-1.34	1274	6.48	0.17
2	0.080427	0.000734	0.002189	0.000020	0.282659	0.000008	-0.76	1238	6.40	0.18
3	0.102160	0.002170	0.002839	0.000075	0.282621	0.000011	-2.20	1329	6.20	0.17
4	0.077076	0.001135	0.002092	0.000026	0.282665	0.000008	-0.53	1223	6.57	0.15
5	0.120020	0.004015	0.003297	0.000119	0.282624	0.000009	-2.14	1325	6.29	0.19
6	0.110845	0.000514	0.002981	0.000016	0.282781	0.000010	3.44	970	6.04	0.23
7	0.094055	0.000715	0.002521	0.000026	0.282736	0.000014	1.91	1067	6.25	0.18
8	0.094693	0.000828	0.002575	0.000025	0.282659	0.000008	-0.81	1240	6.35	0.15
9	0.114848	0.000825	0.003096	0.000026	0.282625	0.000008	-2.08	1321	6.20	0.18
10	0.125748	0.002205	0.003335	0.000055	0.282617	0.000009	-2.40	1341	6.42	0.25
11	0.082600	0.000732	0.002288	0.000019	0.282684	0.000009	0.12	1182	6.50	0.21
12	0.088943	0.001034	0.002452	0.000023	0.282660	0.000008	-0.76	1237	6.20	0.17
13	0.104068	0.002245	0.002794	0.000059	0.282654	0.000009	-1.03	1255	6.41	0.15
14	0.083752	0.000787	0.002223	0.000025	0.282671	0.000008	-0.33	1210	6.56	0.24
15	0.134720	0.000830	0.003494	0.000018	0.282628	0.000008	-2.04	1318	6.03	0.13
16	0.122733	0.001252	0.003184	0.000030	0.282674	0.000009	-0.34	1211	5.75	0.14
17	0.130841	0.001947	0.003340	0.000049	0.282645	0.000010	-1.39	1277	6.15	0.18

-2.4 ~ 3.44, $\varepsilon_{\text{Hf}}(t)$ 加权平均值为 0.75, t_{DM}^{C} 为 1.0 ~ 1.3Ga。与同期的 A 型花岗岩(陂头和温公岩体)特征类似。 $\delta^{18}\text{O}$ 组成相对比较均一, $\delta^{18}\text{O} = 5.75\text{‰} \sim 6.48\text{‰}$, $\delta^{18}\text{O}$ 加权平均值为 6.28‰, 比幔源锆石的值稍高。

4 讨论

4.1 岩石类型

不同类型(I、S-和 A-型)的高演化花岗岩, 由于矿物组合和化学成分都趋近于最低共熔点组分, 呈现相似的地球化学特征(尤其是微量元素行为)因而难以区分(Li *et al.*, 2007; 陈璟元和杨进辉, 2015; Zhang *et al.*, 2017a; 吴福元等, 2017)。大坪花岗斑岩高硅($\text{SiO}_2 > 72\%$), 非常高的 Rb/Sr 比(24.5 ~ 140.2)和非常低的 Zr/Hf(4.1 ~ 11)、Nb/Ta(0.86 ~ 3.78)比值, 及明显的 Eu 负异常(0.04 ~ 0.29), 表明岩石经历了强烈的结晶分异作用。大部分岩石样品表现为弱过铝质(A/CNK = 0.97 ~ 1.10), 只有 2 个样品采集于地表附近, A/CNK 超过 1.1, 结合全岩较高的烧失量, 因而推测这可能是地表风化导致的。其次, 我们没有在薄片中发现 S 型花岗岩的典型过铝质矿物, 如堇青石、白云母、石榴石等(Chappell *et al.*, 1999)。样品的 P_2O_5 的含量很低($< 0.04\%$), 与 SiO_2 相关图上显示的负相关关系, 符合 HW 磷灰石饱和规则(Harrison and Watson modal)并落入 I 型花岗岩的演化趋势线上(Harrison and Watson, 1984; 李献华等, 2007)。此外, 样品中的锆石具有比较低的 O 同位素组成

(~6.28‰), 这与华南典型的 S 型大容山花岗岩也相差甚远。因此, 大坪花岗斑岩不太可能是 S 型花岗岩。

高分异花岗岩与 A 型花岗岩, 特别是铝质 A 型花岗岩就很难区分(Zhang *et al.*, 2017a)。大坪花岗斑岩具高的 Rb、REE、Nb、Ta、Ga、Y 含量, 及高的 $\text{Fe}_2\text{O}_3^{\text{T}}/\text{MgO}$ 比值, 亏损 Ba、Sr、P、Eu。样品的 10000Ga/Al 比值介于 4.96 ~ 6.8, 尽管远高于一般 A 型花岗岩 10000Ga/Al 比值(~2.6), 但仍然落在 A 型花岗岩的范围(图 7a)(Whalen *et al.*, 1987; Eby, 1990; King *et al.*, 2001; Li *et al.*, 2012b; Jiang *et al.*, 2018a, b)。一般而言 A 型花岗岩有着比较高的 Zr + Nb + Ce + Y 含量特征, 如陂头、温公、柯树北岩体, 但是如果岩浆高度演化, 通常会使其低于 A 型花岗岩的判断标准(~ 350×10^{-6})(Landenberger and Collins, 1996; Jiang *et al.*, 2009a; Zhang *et al.*, 2017a)。大坪花岗斑岩的 Zr + Nb + Ce + Y 含量随着采样深度变浅而逐渐降低, 深部岩石分异程度偏低, 有着更高的 Zr + Nb + Ce + Y 含量(~ 412×10^{-6})(图 7b)也符合 A 型花岗岩特征。判断 A 型花岗岩有一个重要特征就是来自于非造山带环境, 而大坪花岗斑岩的样品全部落在板内环境(图 7c, d)。A 型花岗岩还有一个最为重要的特征就是高温。根据锆饱和温度(Watson and Harrison, 1983), 虽然大坪花岗斑岩的锆饱和温度很低(680 ~ 760°C), 但是锆石的 Ti 温度计(Watson *et al.*, 2006), 却记录了非常高的温度(600 ~ 950°C)(图 8)。由于大坪花岗斑岩经历了显著的结晶分异, 随着岩石的深度逐渐变浅, Zr 的含量及 Zr/Hf 比值逐渐降低(图 9), 表明现在全岩 Zr 含量可能并不能代表初始岩浆

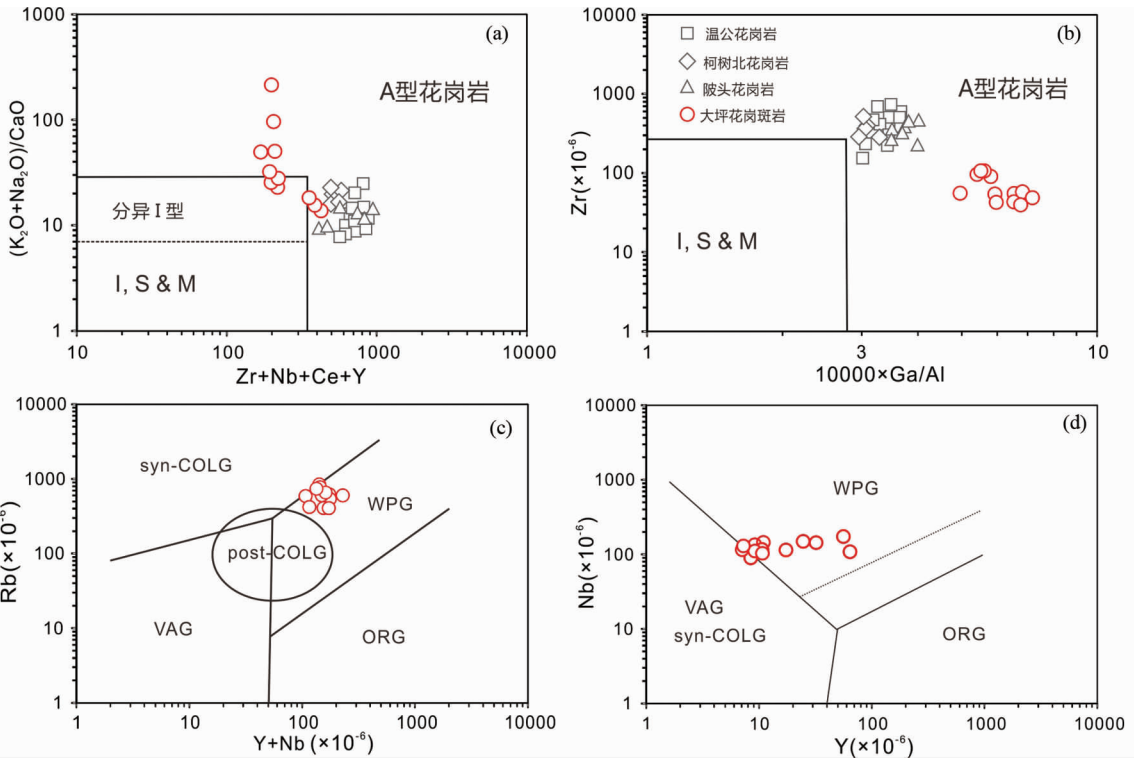


图7 大坪花岗斑岩的 $(K_2O + SiO_2)/CaO$ -Zr + Nb + Ce + Y 图解(a)、Zr-10000Ga/Al 图解(b)、Rb-(Y + Nb) 图解(c) 和 Nb-Y 图解(d) (底图据 Eby, 1990; Whalen *et al.*, 1987)

VAG-火山弧型;Syn-COLG-同碰撞型;WPG-板内型;ORG-洋脊型;Post-COLG-碰撞后型。其他岩体数据据 Gan *et al.* (2017)

Fig.7 Plots of $(K_2O + SiO_2)/CaO$ vs. Zr + Nb + Ce + Y (a), Zr vs. 10000Ga/Al (b), Rb vs. (Y + Nb) (c) and Nb vs. Y (d) for the Daping granite porphyry (base map after Eby, 1990; Whalen *et al.*, 1987)

VAG-volcanic-arc granite; Syn-COLG-syn-collision granite; WPG-within plate granite; ORG-ocean ridge granite; Post-COLG-post collision granite. The data of Wengong, Keshubei and Pitou granites after Gan *et al.* (2017)

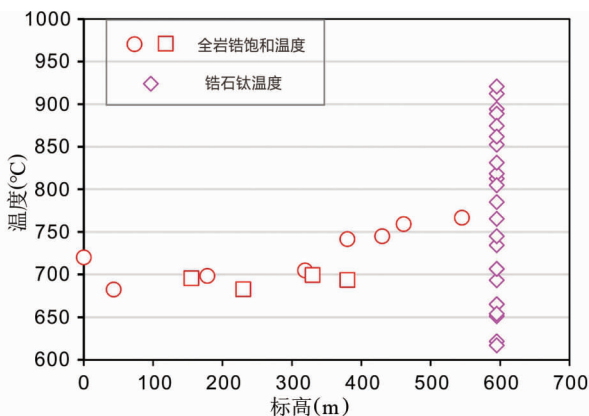


图8 大坪花岗斑岩温度随深度变化图解

Fig.8 Temperature-Depth diagram for the Daping granite porphyry

(Zhang *et al.*, 2018)。而锆石是一种非常稳定的副矿物,贯穿岩浆演化始终,是最有可能反映岩浆真实温度的。因此,我们认为大坪花岗斑岩具有非常高的初始岩浆温度。虽然高分异的I型花岗岩,也能显示许多A型花岗岩的典型特

征,如高的Ga/Al比值等,但是前人研究认为Ga/Al比值和Zr + Nb + Ce + Y含量两个指标综合使用能够提供有效的制约(Zhang *et al.*, 2017a),结合大坪花岗斑岩的高温特征,我们更倾向认为其为A型花岗岩。

4.2 源区特征及其岩石成因

目前有关A型花岗岩的成因存在广泛的争议,特别是其源区性质和形成过程。目前关于其源区主要有以下观点:1)幔源的碱性岩浆直接结晶分异(Eby, 1990; Bonin, 2007); 2)先前经历过部分熔融-岩浆抽离后残留的难熔的下地壳麻粒岩相岩石的再熔(Collins *et al.*, 1982; Whalen *et al.*, 1987; King *et al.*, 1997); 3)浅部地壳底侵作用形成的钙碱性花岗岩的深熔(Creaser *et al.*, 1991); 4)拉斑质岩浆极度分异或者由亏损地幔演化而来的基性下地壳部分熔融(Frost *et al.*, 1999); 5)地壳花岗质岩浆与幔源的基性岩浆混合(Wickham *et al.*, 1996; Yang *et al.*, 2006; Li *et al.*, 2012b; Chen *et al.*, 2016)。另外,同时期南岭地区呈E-W向展布的典型A型花岗岩的成因也一直饱受争议,但是大量幔源岩浆的参与了岩体的形成是被广泛接受的(李献华等,2009)。

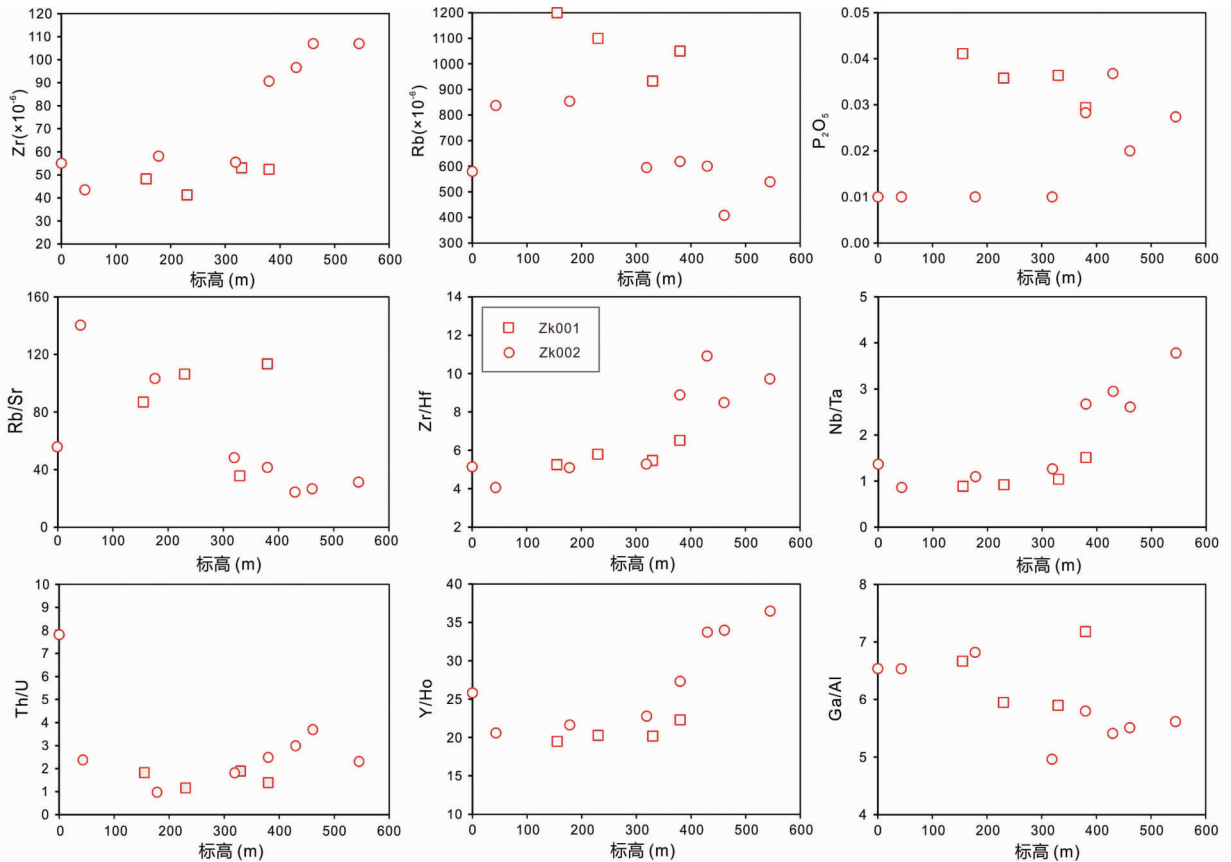


图9 大坪花岗斑岩微量元素含量及比值随深度变化图解

Fig.9 The contents and ratios of trace elements versus depth diagrams for the Daping granite porphyry

大坪花岗斑岩有着非常高的 SiO_2 含量,除了 K_2O 、 Na_2O 、 Al_2O_3 含量变化明显,其它主量元素变化趋势并不明显。野外没有发现相伴生堆晶成因的中-基性岩石, Harker 图解上也没有主量元素连续演化的趋势,因此大坪花岗斑岩似乎很难通过结晶分异形成。第二种解释虽然能形成 A 型花岗岩贫水富钨的特征,却不能解释大坪花岗斑岩 $\text{FeO}/(\text{FeO} + \text{MgO}) > 0.85$ 这种富铁特征 (Creaser *et al.*, 1991)。更为重要的是锆石 Hf-O 同位素二端元混合模拟显示 (图 10),母岩浆主要来源于亏损地幔,且混入了 20% ~ 30% 的地壳物质。因此,大坪岩体也很难直接通过古老的地壳直接熔融形成。那么大坪花岗斑岩形成不外乎两种方式:1) 亏损地幔演化而来的初生基性下地壳部分熔融。大概在新元古代中期 (850 ~ 900Ma) 武夷地区有大规模的幔源岩浆活动 (Li *et al.*, 2010),而这些幔源组分通过底侵方式形成初生地壳,这些基性岩锆石刚好有着与大坪相似的模式年龄 (~ 1.2Ga),大概在 190Ma 左右,发生热事件诱发初生地壳发生部分熔融形成大坪花岗斑岩;2) 幔源岩浆与壳源岩浆混合而成,在 190Ma 左右,岩石圈发生伸展,软流圈地幔减压部分熔融形成拉斑玄武质岩浆诱发部分古老的地壳物质熔融,并与之混合形成大坪花岗岩。另外,区内同时期广泛发育的藩坑组双峰式火山岩及辉长岩岩脉,显示 OIB 的岩石地球化学特征。

这种 OIB 型玄武岩可作为该地区早侏罗世软流圈地幔上涌的岩石学标志 (周金城等, 2005)。因此,我们推测早侏罗世幔源岩浆的上涌不仅提供热量还参与大坪花岗斑岩的形成。

4.3 岩浆-热液过程与 Nb-Ta 成矿

大部分铌-钽花岗岩体都表现出弱过铝质到过铝质和 Nb、Ta 含量随着岩浆演化程度增大而升高的特点 (Dostal *et al.*, 2000; Weyer *et al.*, 2003; Van Lichtervelde *et al.*, 2008),因此,花岗岩中的 Nb、Ta 富集与岩浆体系的高度演化有密切联系。在稀有金属花岗岩演化过程中,随着岩浆演化程度的升高而发生规律性变化,即熔体中的 F、Rb、Li 含量随着岩浆演化程度的升高而增加 (李洁和黄小龙, 2013)。大坪花岗斑岩含有较高的 SiO_2 含量 (高达 77%) 及宽的变化范围,稀土元素分布曲线具有 M 型四分组效应以及明显的 Eu 负异常,这是高分异稀有金属矿化花岗岩的重要标志。

关于花岗岩稀有金属成矿,国际上一直存在较大的争论。部分学者认为稀有金属相关花岗岩的 Nb/Ta 比值显著降低主要与岩浆的结晶分异有关 (Stepanov *et al.*, 2014; Zhang *et al.*, 2017a, 2019)。由于 Nb 在云母中的分配系数大于 Ta,因而随着云母的分异结晶,残余溶体中 Nb 和 Ta 逐渐富集,而 Nb/Ta 比值逐渐降低。而另外部分学者认为稀

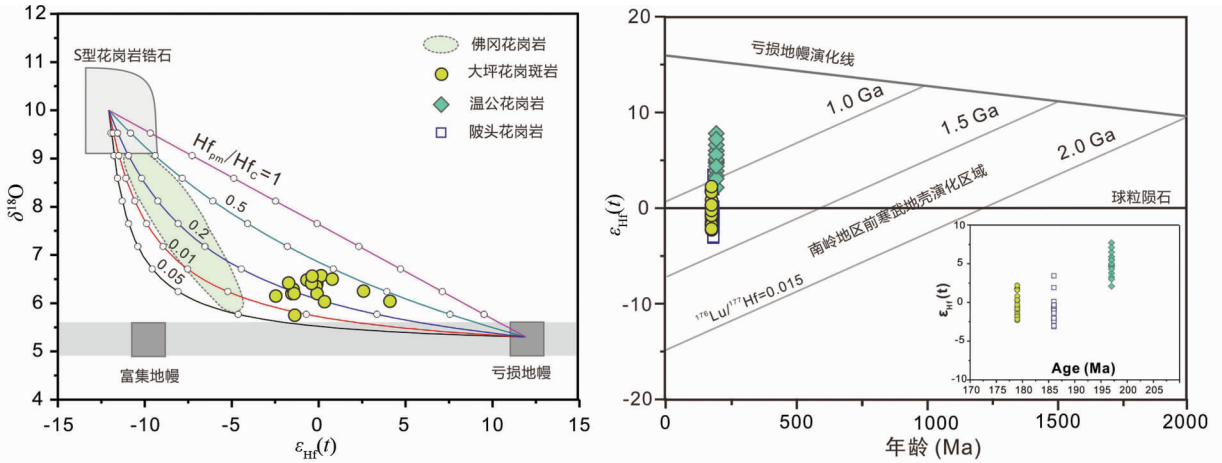


图 10 锆石 Hf-O 同位素相关关系图

点线为地幔和表壳沉积岩来源岩浆二元混合趋势线, Hf_{pm}/Hf_c 代表幔源岩浆与壳源岩浆的 Hf 浓度比, 线上空心圈代表混合比例 (以 10% 为间隔). 地幔端元的锆石 $\epsilon_{Hf} = 12$, $\delta^{18}O = 5.6\text{‰}$ 来源于清湖二长岩, 表壳沉积岩端元的锆石 $\epsilon_{Hf} = -12$, $\delta^{18}O = 10\text{‰}$. 地幔端元及佛冈岩体数据引自李献华等 (2009), 温公岩体和陂头岩体数据引自 Gan *et al.* (2017)

Fig. 10 Plot of Hf vs. O isotopes of zircons from the Daping granite porphyry

The dotted lines denote the two-component mixing trends between the mantle and supercrust derived magmas. Hf_{pm}/Hf_c is the ratio of Hf concentration in the parental mantle magma (pm) over crustal (c) melt indicated for each curves, and the small open circles on the curves represent 10% mixing increments by assuming the mantle zircon has $\epsilon_{Hf} = 12$ and $\delta^{18}O = 5.6\text{‰}$; the supercrustal zircon has $\epsilon_{Hf} = -12$ and $\delta^{18}O = 10\text{‰}$. The data of the mantle end member and the Fogang granite is after Li *et al.* (2009), and the data of the Wengong granite and Pitou granite is after Gan *et al.* (2017)

有金属花岗岩有着极低的 Nb/Ta 比值 (< 5), 模拟计算表明高达 90% 的分离结晶才能形成如此低的 Nb/Ta 比值, 显然这在自然系统中是不可能的, 而亚固相下的岩浆-热液过程在再次富集稀有金属元素和分异 Nb-Ta 过程中起了很重要的作用 (Ballouard *et al.*, 2016). Nb 和 Ta 被称为高场强元素, 一般认为在热液中极其不活动的, 但是最近的实验岩石学研究表明, 在富氟的溶液体系中 Nb 和 Ta 是可以与氟形成络合物而被稳定迁移的 (Timofeev *et al.*, 2015, 2017)。

以 ZK001 为例 (图 9), 从下往上我们选择了一条剖面, 我们发现随着标高变小, Rb 含量及 Rb/Sr 比值显著升高, Nb/Ta, Zr/Hf, Th/U 比值逐渐降低, 而 Nb 和 Ta 的含量逐渐升高。在几百米的深度我们并没有观察到明显的结晶分异现象, 因而我们更倾向认为 Nb 和 Ta 的富集与分异更多受控于岩浆-热液过程。大坪花岗岩全岩包含了较高的 F 含量 (高达 0.8%, 未发表数据), 及野外露头 and 显微镜下都能观察到萤石, 均表明岩石具有高的氟含量。全岩高的 Y/Ho 比值也说明流体与岩浆的相互作用 (陈璟元和杨进辉, 2015)。因此, 我认为岩石高程度演化是大坪花岗斑岩成矿元素以及挥发组份高度富集的重要控制因素。而晚期富氟的流体出熔及向上迁移对稀有金属再次富集及 Nb/Ta 分异具有很重要的作用。

4.4 构造启示意义

南岭燕山早期的火成岩是华南印支期造山运动后的板内岩浆活动, 在 200 ~ 70Ma 期间出现了以玄武岩和 A 型酸性

火山岩及其侵入相辉长岩和 A 型花岗岩的“双峰式”火成岩组合为特征, 这些岩石分布于一个近 E-W 向展布的区域, 岩石组合表明它们形成于伸展拉张背景 (图 1a) (李献华等, 2007)。这些火成岩虽规模小但分布广泛, 包括湘南宁远-新田碱性玄武岩 (Li *et al.*, 2004)、湘东南宜章长城岭拉斑玄武岩 (赵振华等, 1998)、赣南龙南东坑-临江盆地和寻乌白面石-菖蒲盆地拉斑玄武岩 (陈培荣等, 1999; Gan *et al.*, 2017)、赣中吉安安塘碱性玄武岩 (王岳军等, 2004) 和闽西南永定盆地拉斑玄武岩 (周金城等, 2005)。这些玄武岩均显示出洋岛玄武岩 (OIB) 的地球化学和同位素组成特征。目前报道的与双峰式火山岩相伴生的辉长岩与 A 型花岗岩 (包括寨北、柯树北、温公、大坪 A 型花岗岩) 同样显示相对亏损的同位素特征, 表明这时期存在大量的软流圈地幔物质上涌。由于研究区刚好处于古特提斯构造域与古太平洋构造域交界部位, 而三叠纪-侏罗纪时期刚好处于两大构造域转换时期 (张岳桥等, 2009; 舒良树, 2012; Wang *et al.*, 2013), 所以关于其成因存在不同观点。例如, 部分学者认为此岩石组合是继三叠纪印支地块与华南地块碰撞造山 (Carter *et al.*, 2001) 以后的一种后造山大陆裂解地球动力背景下的产物, 持续到早侏罗世 (陈培荣等, 2002; 付建明等, 2004; Chen *et al.*, 2008)。而部分学者提出质疑, 广泛出露三叠纪的 A 型花岗岩的时代为 229 ~ 215Ma (王丽娟等, 2007; Zhao *et al.*, 2013; Gan *et al.*, 2017), 可能标志碰撞后广泛的伸展活动, 而 215Ma 以后伸展已经结束, 伸展很难持续到 ~ 170Ma, 况且在全球的典型的造山带也几乎没有碰撞后伸展持续近 50Ma 的先例。Li and Li (2007) 认为华南广泛的陆内变形与

三叠-白垩纪的岩浆活动可能都受控于古太平洋的俯冲作用, 继而提出了一个平板俯冲的模型, 在三叠纪古太平洋板块向西俯冲形成 1300 km 范围的陆内变形, 大概在晚侏罗世末, 由于板片后撤, 导致平坦的板片发生破坏或撕裂, 形成了广泛的晚中生代岩浆活动。由于没有在华南发现板片熔融的埃达克岩及弧相关与非弧相关的岩石组合, 晚侏罗世的岩浆岩基本为板内环境, 因此这个模型也遭到大家的广泛质疑。Zhou *et al.* (2006) 提出古太平洋板块两阶段模型, 侏罗纪的岩浆活动主要与初始俯冲相关, 属于板内阶段; 但是随后的白垩纪岩浆活动, 才是活动大陆边缘环境。因此, 部分学者认为 200 ~ 170Ma 的岩浆活动可能与俯冲初始阶段相关, 古太平洋板块俯冲的远程效应导致先存在的断裂活化, 诱导南岭局部大规模的伸展, 并伴随着大量的软流圈地幔上涌(谢昕等, 2005; Jiang *et al.*, 2009a; 余心起等, 2009; He *et al.*, 2010; Yu *et al.*, 2010; Gan *et al.*, 2017; Zhou *et al.*, 2018)。对此很多学者也提出质疑, 认为 NE 向俯冲如何形成近 W-E 的伸展作用, 在几何学上很难实现。总之, 就像上面讨论, 晚三叠世的 A 型花岗岩形成于碰撞后伸展背景, 属于古特提斯构造域。而晚侏罗-早白垩世 A 型花岗岩主要形成与弧后伸展环境, 受控于古太平洋构造域(邱检生等, 1999; Zhou *et al.*, 2006; 肖娥等, 2007; Wang *et al.*, 2011; 林清茶等, 2011; Sun *et al.*, 2012; Chen *et al.*, 2013; Gan *et al.*, 2017)。而 200 ~ 170Ma 近 E-W 向岩浆活动与构造伸展, 可能标志着两大构造域在早侏罗世发生转折, 但是关于其成因需要我们进一步的工作。

5 结论

(1) 大坪花岗岩斑岩 SIMS 锆石 U-Pb 年龄和 LA-ICP-MS 锆石 U-Pb 年龄分别为 186.7 ± 1.2 Ma 和 190.7 ± 1.1 Ma, 是区内首次报道早侏罗世 A 型花岗岩 Nb-Ta 成矿事件。

(2) 大坪花岗岩斑岩的 Hf-O 同为素揭示其源区大概 70% ~ 80% 软流圈地幔物质, 且混合或混染 20% ~ 30% 的地壳物质。

(3) 大坪花岗岩斑岩与闽西南地区同时期的火山岩, 如藩坑组双峰式火山岩, 在空间上可与前人提出的“南岭山脉早侏罗世发育的东西向裂谷岩浆岩带(OIB 型玄武岩、辉长岩和 A 型花岗岩组合)”相对应, 是该裂谷带向东的延伸。

致谢 野外地质工作得到了中国冶金地质总局第二地质勘查院叶盛源工程师的帮助; 中国科学院海洋研究所孙卫东研究员对本文给予了指导; 中国科学院广州地球化学研究所夏小平研究员及中国冶金地质总局山东局测试中心林培军、王继林等工程师对测试提供了帮助; 审稿人及编辑部老师对本文成稿提出了修改意见; 在此一并表示衷心感谢!

References

- Ballouard C, Poujol M, Boulvais P, Branque Y, Tartèse R and Vigneresse JL. 2016. Nb-Ta fractionation in peraluminous granites: A marker of the magmatic-hydrothermal transition. *Geology*, 44(3): 231 - 234
- Blichert-Toft J and Albarède F. 1997. The Lu-Hf isotope geochemistry of chondrites and the evolution of the mantle-crust system. *Earth and Planetary Science Letters*, 148(1-2): 243 - 258
- Bonin B. 2007. A-type granites and related rocks: Evolution of a concept, problems and prospects. *Lithos*, 97(1-2): 1 - 29
- Carter A, Roques D, Bristow C and Kinny P. 2001. Understanding Mesozoic accretion in Southeast Asia: Significance of Triassic thermotectonism (Indosinian orogeny) in Vietnam. *Geology*, 29(3): 211 - 214
- Chappell BW. 1999. Aluminium saturation in I- and S-type granites and the characterization of fractionated haplogranites. *Lithos*, 46(3): 535 - 551
- Chen CH, Lee CY and Shinjo R. 2008. Was there Jurassic paleo-Pacific subduction in South China? Constraints from $^{40}\text{Ar}/^{39}\text{Ar}$ dating, elemental and Sr-Nd-Pb isotopic geochemistry of the Mesozoic basalts. *Lithos*, 106(1-2): 83 - 92
- Chen JY, Yang JH, Zhang JH, Sun JF and Wilde SA. 2013. Petrogenesis of the Cretaceous Zhangzhou batholith in southeastern China: Zircon U-Pb age and Sr-Nd-Hf-O isotopic evidence. *Lithos*, 162 - 163: 140 - 156
- Chen JY and Yang JH. 2015. Petrogenesis of the Fogang highly fractionated I-type granitoids: Constraints from Nb, Ta, Zr and Hf. *Acta Petrologica Sinica*, 31(3): 846 - 854 (in Chinese with English abstract)
- Chen PR, Kong XG, Ni QS, Zhang BT and Liu CS. 1999. Ascertainment and implication of the Early Yanshanian bimodal volcanic associations from South Jiangxi Province. *Geological Review*, 45 (Suppl. 1): 734 - 741 (in Chinese with English abstract)
- Chen PR, Hua RM, Zhang BT, Lu JJ and Fan CF. 2002. Early Yanshanian post-orogenic granitoids in the Nanling region: Petrological constraints and geodynamic settings. *Science in China (Series D)*, 45(8): 755 - 768
- Chen YX, Li H, Sun WD, Ireland T, Tian XF, Hu YB, Yang WB, Chen C and Xu DR. 2016. Generation of Late Mesozoic Qianlishan A₂-type granite in Nanling Range, South China: Implications for Shizhuyuan W-Sn mineralization and tectonic evolution. *Lithos*, 266 - 267: 435 - 452
- Collins WJ, Beams SD, White AJR and Chappell BW. 1982. Nature and origin of A-type granites with particular reference to southeastern Australia. *Contributions to Mineralogy and Petrology*, 80(2): 189 - 200
- Creaser RA, Price RC and Wormald RJ. 1991. A-type granites revisited: Assessment of a residual-source model. *Geology*, 19(2): 163 - 166
- Dostal J and Chatterjee AK. 2000. Contrasting behaviour of Nb/Ta and Zr/Hf ratios in a peraluminous granitic pluton (Nova Scotia, Canada). *Chemical Geology*, 163(1-4): 207 - 218
- Eby GN. 1990. The A-type granitoids: A review of their occurrence and chemical characteristics and speculations on their petrogenesis. *Lithos*, 26(1-2): 115 - 134
- Frost CD, Frost BR, Chamberlain KR and Edwards BR. 1999. Petrogenesis of the 1.43Ga Sherman Batholith, SE Wyoming, USA: A reduced, Rapakivi-type anorogenic granite. *Journal of Petrology*, 40(12): 1771 - 1802
- Fu JM, Ma CQ, Xie CF, Zhang YM and Peng SB. 2004. Geochemistry and tectonic setting of Xishan aluminous A-type granitic volcanic-intrusive complex, southern Hunan. *Journal of Earth Sciences and Environment*, 26(4): 15 - 23 (in Chinese with English abstract)
- Gan CS, Wang YJ, Cai YF, Liu HC, Zhang YZ, Song JJ and Guo XF.

2016. The petrogenesis and tectonic implication of Wengong intrusion in the Nanling Range. *Earth Science*, 41(1): 17–34 (in Chinese with English abstract)
- Gan CS, Wang YJ, Qian X, Bi MW and He HY. 2017. Constraints of the Xialan gabbroic intrusion in the eastern Nanling Range on the Early Jurassic intra-continental extension in eastern South China. *Journal of Asian Earth Sciences*, 145: 576–590
- Griffin WL, Belousova EA, Shee SR, Pearson NJ and O'Reilly SY. 2004. Archean crustal evolution in the northern Yilgarn Craton: U-Pb and Hf-isotope evidence from detrital zircons. *Precambrian Research*, 131(3–4): 231–282
- Harrison TM and Watson EB. 1984. The behavior of apatite during crustal anatexis; Equilibrium and kinetic considerations. *Geochimica et Cosmochimica Acta*, 48(7): 1467–1477
- He ZY, Xu XS and Niu YL. 2010. Petrogenesis and tectonic significance of a Mesozoic granite-syenite-gabbro association from inland South China. *Lithos*, 119(3–4): 621–641
- Jahn BM, Chen PY and Yen TP. 1976. Rb-Sr ages of granitic rocks in southeastern China and their tectonic significance. *Geological Society of America Bulletin*, 87(5): 763–776
- Jiang N, Zhang SQ, Zhou WG and Liu YS. 2009a. Origin of a Mesozoic granite with A-type characteristics from the North China craton: Highly fractionated from I-type magmas? *Contributions to Mineralogy and Petrology*, 158(1): 113–130
- Jiang XY, Li H, Ding X, Wu K, Guo J, Liu JQ and Sun WD. 2018a. Formation of A-type granites in the Lower Yangtze River Belt: A perspective from apatite geochemistry. *Lithos*, 304–307: 125–134
- Jiang XY, Luo JC, Guo J, Wu K, Zhang ZK, Sun WD and Xia XP. 2018b. Geochemistry of I- and A-type granites of the Qingyang-Jiuhuashan complex, eastern China: Insights into early cretaceous multistage magmatism. *Lithos*, 316–317: 278–294
- Jiang YH, Jiang SY, Dai BZ, Liao SY, Zhao KD and Ling HF. 2009b. Middle to Late Jurassic felsic and mafic magmatism in southern Hunan Province, Southeast China: Implications for a continental arc to rifting. *Lithos*, 107(3–4): 185–204
- King PL, White AJR, Chappell BW and Allen CM. 1997. Characterization and origin of aluminous A-type granites from the Lachlan Fold Belt, Southeastern Australia. *Journal of Petrology*, 38(3): 371–391
- King PL, Chappell BW, Allen CM and White AJR. 2001. Are A-type granites the high-temperature felsic granites? Evidence from fractionated granites of the Wangrah Suite. *Australian Journal of Earth Sciences*, 48(4): 501–514
- Landenberger B and Collins WJ. 1996. Derivation of A-type granites from a dehydrated charnockitic lower crust: Evidence from the Chaelundi Complex, eastern Australia. *Journal of Petrology*, 37(1): 145–170
- Li CY, Zhang H, Wang FY, Liu JQ, Sun YL, Hao XL, Li YL and Sun WD. 2012a. The formation of the Dabaoshan porphyry molybdenum deposit induced by slab rollback. *Lithos*, 150: 101–110
- Li H, Ling MX, Li CY, Zhang H, Ding X, Yang XY, Fan WM, Li YL and Sun WD. 2012b. A-type granite belts of two chemical subgroups in central eastern China: Indication of ridge subduction. *Lithos*, 150: 26–36
- Li H, Ling MX, Ding X, Zhang H, Li CY, Liu DY and Sun WD. 2014a. The geochemical characteristics of Haiyang A-type granite complex in Shandong, eastern China. *Lithos*, 200–201: 142–156
- Li H, Watanabe K and Yonezu K. 2014b. Geochemistry of A-type granites in the Huangshaping polymetallic deposit (South Hunan, China): Implications for granite evolution and associated mineralization. *Journal of Asian Earth Sciences*, 88: 149–167
- Li J and Huang XL. 2013. Mechanism of Ta-Nb enrichment and magmatic evolution in the Yashan granites, Jiangxi Province, South China. *Acta Petrologica Sinica*, 29(12): 4311–4322 (in Chinese with English abstract)
- Li XH, Chen ZG, Liu DY and Li WX. 2003. Jurassic gabbro-granite-syenite suites from southern Jiangxi Province, SE China: Age, origin, and tectonic significance. *International Geology Review*, 45(10): 898–921
- Li XH, Chung SL, Zhou HW, Lo CH, Liu Y and Chen CH. 2004. Jurassic intraplate magmatism in southern Hunan-eastern Guangxi: $^{40}\text{Ar}/^{39}\text{Ar}$ dating, geochemistry, Sr-Nd isotopes and implications for the tectonic evolution of SE China. In: Malpas J, Fletcher CJ, Aitchison JC and Ali J (eds.). *Aspects of the Tectonic Evolution of China*. Geological Society, London, Special Publications, 226: 193–215
- Li XH, Li ZX, Li WX, Liu Y, Yuan C, Wei GJ and Qi CS. 2007. U-Pb zircon, geochemical and Sr-Nd-Hf isotopic constraints on age and origin of Jurassic I- and A-type granites from central Guangdong, SE China: A major igneous event in response to foundering of a subducted flat-slab? *Lithos*, 96(1–2): 186–204
- Li XH, Li WX and Li ZX. 2007. On the genetic classification and tectonic implications of the Early Yanshanian granitoids in the Nanling Range, South China. *Chinese Science Bulletin*, 52(14): 1873–1885
- Li XH, Liu Y, Li QL, Guo CH and Chamberlain KR. 2009. Precise determination of Phanerozoic zircon Pb/Pb age by multicollector SIMS without external standardization. *Geochemistry, Geophysics, Geosystems*, 10(4): Q04010
- Li XH, Li WX, Wang XC, Li QL, Liu Y and Tang GQ. 2009. Role of mantle-derived magma in genesis of Early Yanshanian granites in the Nanling Range, South China: In situ zircon Hf-O isotopic constraints. *Science in China (Series D)*, 52(9): 1262–1278
- Li Z, Qiu JS and Yang XM. 2014c. A review of the geochronology and geochemistry of Late Yanshanian (Cretaceous) plutons along the Fujian coastal area of southeastern China: Implications for magma evolution related to slab break-off and rollback in the Cretaceous. *Earth-Science Reviews*, 128: 232–248
- Li ZX and Li XH. 2007. Formation of the 1300-km-wide intracontinental orogen and postorogenic magmatic province in Mesozoic South China: A flat-slab subduction model. *Geology*, 35(2): 179–182
- Li ZX, Li XH, Wartho JA, Clark C, Li WX, Zhang CL and Bao CD. 2010. Magmatic and metamorphic events during the Early Paleozoic Wuyi-Yunkai orogeny, southeastern South China: New age constraints and pressure-temperature conditions. *Geological Society of America Bulletin*, 122(5–6): 772–793
- Lin J, Liu YS, Yang YH and Hu ZC. 2016. Calibration and correction of LA-ICP-MS and LA-MC-ICP-MS analyses for element contents and isotopic ratios. *Solid Earth Sciences*, 1(1): 5–27
- Lin QC, Cheng XW, Zhang YQ and Wang FY. 2011. Evolution of granitoids in the active continental margin: A case study of the Fuzhou compound complex. *Acta Geologica Sinica*, 85(7): 1128–1133 (in Chinese with English abstract)
- Liu YC, Li JK, Zou TR, Jiang SY, Hu MY and Chen ZY. 2017. Enrichment characteristics of Nb and Ta of Daping granite porphyry in Yongding, Fujian Province. *Mineral Deposits*, 36(1): 143–157 (in Chinese with English abstract)
- Ma JQ and Wang WT. 1993. Basic characteristics and the stratigraphic-time basis of Middle and Lower Proterozoic metamorphic rocks in the Yongding area of Fujian Province. *Geology of Fujian*, 12(4): 268–279 (in Chinese with English abstract)
- Maniar PD and Piccoli PM. 1989. Tectonic discrimination of granitoids. *Geological society of America bulletin*, 101(5): 635–643
- McDonough WF and Sun SS. 1995. The composition of the Earth. *Chemical geology*, 120(3–4): 223–253
- Mao JW, Cheng YB, Chen MH and Pirajno F. 2013. Major types and time-space distribution of Mesozoic ore deposits in South China and their geodynamic settings. *Mineralium Deposita*, 48(3): 267–294
- Peccerillo A and Taylor SR. 1976. Geochemistry of Eocene calc-alkaline volcanic rocks from the Kastamonu area, northern Turkey. *Contributions to Mineralogy and Petrology*, 58(1): 63–81
- Qiu JS, Wang DZ and McInnes BAI. 1999. Geochemistry and petrogenesis of the I- and A-type composite granite masses in the coastal area of Zhejiang and Fujian provinces. *Acta Petrologica Sinica*, 15(2): 237–246 (in Chinese with English abstract)
- Scherer E, Münker C and Mezger K. 2001. Calibration of the lutetium-hafnium clock. *Science*, 293(5530): 683–687

- Shu LS, Zhou XM, Deng P, Yu XQ, Wang B and Zu FP. 2004. Geological features and tectonic evolution of Meso-Cenozoic basins in southeastern China. *Geological Bulletin of China*, 23(9-10): 876-884 (in Chinese with English abstract)
- Shu LS. 2006. Predevonian tectonic evolution of South China; From Cathaysian block to Caledonian Period folded orogenic belt. *Geological Journal of China Universities*, 12(4): 418-431 (in Chinese with English abstract)
- Shu LS. 2012. An analysis of principal features of tectonic evolution in South China Block. *Geological Bulletin of China*, 31(7): 1035-1053 (in Chinese with English abstract)
- Stepanov A, Mavrogenes JA, Meffre S and Davidson P. 2014. The key role of mica during igneous concentration of tantalum. *Contributions to Mineralogy Petrology*, 167: 1009
- Sun WD, Ding X, Hu YH and Li XH. 2007. The golden transformation of the Cretaceous plate subduction in the West Pacific. *Earth and Planetary Science Letters*, 262(3-4): 533-542
- Sun WD, Yang XY, Fan WM and Wu FY. 2012. Mesozoic large scale magmatism and mineralization in South China; Preface. *Lithos*, 150: 1-5
- Timofeev A, Migdisov AA and Williams-Jones AE. 2015. An experimental study of the solubility and speciation of niobium in fluoride-bearing aqueous solutions at elevated temperature. *Geochimica et Cosmochimica Acta*, 158: 103-111
- Timofeev A, Migdisov AA and Williams-Jones AE. 2017. An experimental study of the solubility and speciation of tantalum in fluoride-bearing aqueous solutions at elevated temperature. *Geochimica et Cosmochimica Acta*, 197: 294-304
- Van Lichtervelde M, Grégoire M, Linnen RL, Béziat D and Salvi S. 2008. Trace element geochemistry by laser ablation ICP-MS of micas associated with Ta mineralization in the Tanco pegmatite, Manitoba, Canada. *Contributions to Mineralogy and Petrology*, 155(6): 791-806
- Vervoort JD and Blichert-Toft J. 1999. Evolution of the depleted mantle: Hf isotope evidence from juvenile rocks through time. *Geochimica et Cosmochimica Acta*, 63(3-4): 533-556
- Wang FY, Ling MX, Ding X, Hu YH, Zhou JB, Yang XY, Liang HY, Fan WM and Sun WD. 2011. Mesozoic large magmatic events and mineralization in SE China; Oblique subduction of the Pacific plate. *International Geology Review*, 53(5-6): 704-726
- Wang LJ, Yu JH, Xu XS, Xie L, Qiu JS and Sun T. 2007. Formation age and origin of the Gutian-Xiaotao granitic complex in the southwestern Fujian Province, China. *Acta Petrologica Sinica*, 23(6): 1470-1484 (in Chinese with English abstract)
- Wang YJ, Liao CL, Fan WM and Peng TP. 2004. Early Mesozoic OIB-type alkaline basalt in central Jiangxi Province and its tectonic implications. *Geochimica*, 33(2): 109-117 (in Chinese with English abstract)
- Wang YJ, Fan WM, Zhang GW and Zhang YH. 2013. Phanerozoic tectonics of the South China Block: Key observations and controversies. *Gondwana Research*, 23(4): 1273-1305
- Watson EB and Harrison TM. 1983. Zircon saturation revisited: Temperature and composition effects in a variety of crustal magma types. *Earth and Planetary Science Letters*, 64(2): 295-304
- Watson EB, Wark DA and Thomas JB. 2006. Crystallization thermometers for zircon and rutile. *Contributions to Mineralogy and Petrology*, 151(4): 413-433
- Weyer S, Munker C and Mezger K. 2003. Nb/Ta, Zr/Hf and REE in the depleted mantle: Implications for the differentiation history of the crust-mantle system. *Earth and Planetary Science Letters*, 205(3-4): 309-324
- Whalen JB, Currie KL and Chappell BW. 1987. A-type granites: Geochemical characteristics, discrimination and petrogenesis. *Contributions to Mineralogy and Petrology*, 95(4): 407-419
- Wickham SM, Alberts AD, Zanvilevich AN, Litvinovsky BA, Bindeman IN and Schauble EA. 1996. A stable isotope study of anorogenic magmatism in East Central Asia. *Journal of Petrology*, 37(5): 1063-1095
- Wu FY, Liu XC, Ji WQ, Wang JM and Yang L. 2017. Highly fractionated granites: Recognition and research. *Science China (Earth Sciences)*, 60(7): 1201-1219
- Xiao E, Qiu JS, Xu XS, Jiang SY, Hu J and Li Z. 2007. Geochronology and geochemistry of the Yaokeng alkaline granitic pluton in Zhejiang Province; Petrogenetic and tectonic implications. *Acta Petrologica Sinica*, 23(6): 1431-1440 (in Chinese with English abstract)
- Xie X, Xu XS, Zou HB, Jiang SY, Zhang M and Qiu JS. 2005. Early J₂ basalts in SE China: Incipience of large-scale Late Mesozoic magmatism. *Science in China (Series D)*, 49: 796-815
- Xing GF, Lu QD, Chen R, Zhang ZY, Nie TC, Li LM, Huang JL and Lin M. 2018. Study on the ending time of Late Mesozoic tectonic regime transition in South China; Comparing to the Yanshan area in North China. *Acta Geologica Sinica*, 82(4): 451-463 (in Chinese with English abstract)
- Xu MH. 1993. Basic characteristics of Early Jurassic volcanic-eruption basin in Wuhu, Yongding County, Fujian Province. *Geology of Fujian*, 12(3): 202-209 (in Chinese with English abstract)
- Yang JH, Wu FY, Chung SL, Wilde SA and Chu MF. 2006. A hybrid origin for the Qianshan A-type granite, Northeast China: Geochemical and Sr-Nd-Hf isotopic evidence. *Lithos*, 89(1-2): 89-106
- Yu XQ, Wu GG, Zhao XX, Gao JF, Di YJ, Zheng Y, Dai YP, Li CL and Qiu JT. 2010. The Early Jurassic tectono-magmatic events in southern Jiangxi and northern Guangdong provinces, SE China: Constraints from the SHRIMP zircon U-Pb dating. *Journal of Asian Earth Sciences*, 39(5): 408-422
- Yu XQ, Di YJ, Wu GG, Zhang D, Zheng Y and Dai YP. 2009. The Early Jurassic magmatism in northern Guangdong Province, southeastern China: Constraints from SHRIMP zircon U-Pb dating of Xialan complex. *Science in China (Series D)*, 52(4): 471-483
- Zhang CC, Sun WD, Wang JT, Zhang LP, Sun SJ and Wu K. 2017c. Oxygen fugacity and porphyry mineralization: A zircon perspective of Dexing porphyry Cu deposit, China. *Geochimica et Cosmochimica Acta*, 206: 343-363
- Zhang LP, Zhang RQ, Hu YB, Liang JL, Ouyang ZX, He JJ, Chen YX, Guo J and Sun WD. 2017a. The formation of the Late Cretaceous Xishan Sn-W deposit, South China: Geochronological and geochemical perspectives. *Lithos*, 290-291: 253-268
- Zhang LP, Zhang RQ, Wu K, Chen YX, Li CY, Hu YB, He JJ, Liang JL and Sun WD. 2018. Late Cretaceous granitic magmatism and mineralization in the Yingwuling W-Sn deposit, South China: Constraints from zircon and cassiterite U-Pb geochronology and whole-rock geochemistry. *Ore Geology Reviews*, 96: 115-129
- Zhang LP, Zhang RQ, Chen YX, Sun SJ, Liang JL and Sun WD. 2019. Geochronology and geochemistry of the Late Cretaceous Xinpeng granitic intrusion, South China: Implication for Sn-W mineralization. *Ore Geology Reviews*, 113: 103075, doi: 10.1016/j.oregeorev.2019.103075
- Zhang RQ, Lu JJ, Lehmann B, Li CY, Li GL, Zhang LP, Guo J and Sun WD. 2017b. Combined zircon and cassiterite U-Pb dating of the Piaotang granite-related tungsten-tin deposit, southern Jiangxi tungsten district, China. *Ore Geology Reviews*, 82: 268-284
- Zhang YQ, Xu XB, Jia D and Shu LS. 2009. Deformation record of the change from Indosinian collision-related tectonic system to Yanshanian subduction-related tectonic system in South China during the Early Mesozoic. *Earth Science Frontiers*, 16(1): 234-247 (in Chinese with English abstract)
- Zhang ZJ and Zuo RG. 2015. Tectonic evolution of southwestern Fujian Province and spatial-temporal distribution regularity of mineral deposits. *Acta Petrologica Sinica*, 31(1): 217-229 (in Chinese with English abstract)
- Zhao KD, Jiang SY, Chen WF, Chen PR and Ling HF. 2013. Zircon U-Pb chronology and elemental and Sr-Nd-Hf isotope geochemistry of two Triassic A-type granites in South China: Implication for petrogenesis and Indosinian transtensional tectonism. *Lithos*, 160-161: 292-306
- Zhao ZH, Bao ZW and Zhang BY. 1998. Geochemistry of the Mesozoic

- basaltic rocks in southern Hunan Province. *Science China (Series D)*, 41: 102–112
- Zhou JC and Chen R. 2001. Geochemistry of late Mesozoic interaction between crust and mantle in southeastern Fujian Province. *Geochimica*, 30(6): 547–558 (in Chinese with English abstract)
- Zhou JC, Jiang SY, Wang XL, Yang JQ and Zhang MQ. 2006. Study on litho-geo-chemistry of Middle Jurassic basalts from southern China represented by the Fankeng basalts from Yongding of Fujian Province. *Science in China (Series D)*, 49(10): 1020–1031
- Zhou XM, Sun T, Shen WZ, Shu LS and Niu YL. 2006. Petrogenesis of Mesozoic granitoids and volcanic rocks in South China: A response to tectonic evolution. *Episodes*, 29(1): 26–33
- Zhou ZM, Ma CQ, Wang LX, Chen SG, Xie CF, Li Y and Liu W. 2018. A source-depleted Early Jurassic granitic pluton from South China: Implication to the Mesozoic juvenile accretion of the South China crust. *Lithos*, 300–301: 278–290
- Zhu WG, Zhong H, Li XH, He DF, Song XY, Ren T, Chen ZQ, Sun HS and Liao JQ. 2010. The Early Jurassic mafic-ultramafic intrusion and A-type granite from northeastern Guangdong, SE China: Age, origin, and tectonic significance. *Lithos*, 119(3–4): 313–329
- 附中文参考文献**
- 陈璟元, 杨进辉. 2015. 佛冈高分异 I 型花岗岩的成因: 来自 Nb-Ta-Zr-Hf 等元素的制约. *岩石学报*, 31(3): 846–854
- 陈培荣, 华仁民, 章邦桐, 陆建军, 范春方. 2002. 南岭燕山早期后造山花岗岩类: 岩石学制约和地球动力学背景. *中国科学(D 辑)*, 32(4): 279–289
- 陈培荣, 孔兴功, 倪琦生, 章邦桐, 刘昌实. 1999. 赣南燕山早期双峰式火山岩的厘定和意义. *地质论评*, 45(增 1): 734–741
- 付建明, 马昌前, 谢才富, 张业明, 彭松柏. 2004. 湘南西山铝质 A 型花岗质火山-侵入杂岩的地球化学及其形成环境. *地球科学与环境学报*, 26(4): 15–23
- 甘成势, 王岳军, 蔡永丰, 刘汇川, 张玉芝, 宋菁菁, 郭小飞. 2016. 南岭地区温公岩体的岩石成因及其构造指示. *地球科学*, 41(1): 17–34
- 李洁, 黄小龙. 2013. 江西雅山花岗岩岩浆演化及其 Ta-Nb 富集机制. *岩石学报*, 29(12): 4311–4322
- 李献华, 李武显, 李正祥. 2007. 再论南岭燕山早期花岗岩的成因类型与构造意义. *科学通报*, 52(9): 981–991
- 李献华, 李武显, 王选策, 李秋立, 刘宇, 唐国强. 2009. 幔源岩浆在南岭燕山早期花岗岩形成中的作用: 锆石原位 Hf-O 同位素制约. *中国科学(D 辑)*, 39(7): 872–887
- 林清茶, 程雄卫, 张玉泉, 汪方跃. 2011. 活动大陆边缘花岗岩类演化——以福州复式岩体为例. *地质学报*, 85(7): 1128–1133
- 刘永超, 李建康, 邹天人, 江善元, 胡明月, 陈振宇. 2017. 福建永定大坪花岗岩斑岩体的铌钽富集特征研究. *矿床地质*, 36(1): 143–157
- 马金清, 王文腾. 1993. 福建永定地区下、中元古界变质岩基本特征及地层时代依据. *福建地质*, 12(4): 268–279
- 邱检生, 王德滋, McInnes BIA. 1999. 浙闽沿海地区 I 型-A 型复合花岗岩体的地球化学及成因. *岩石学报*, 15(2): 237–246
- 舒良树, 周新民, 邓平, 余心起, 王彬, 祖辅平. 2004. 中国东南部中、新生代盆地特征与构造演化. *地质通报*, 23(9–10): 876–884
- 舒良树. 2006. 华南前泥盆纪构造演化: 从华夏地块到加里东期造山带. *高校地质学报*, 12(4): 418–431
- 舒良树. 2012. 华南构造演化的基本特征. *地质通报*, 31(7): 1035–1053
- 王丽娟, 于津海, 徐夕生, 谢磊, 邱检生, 孙涛. 2007. 闽西南古田-小陶花岗质杂岩体的形成时代和成因. *岩石学报*, 23(6): 1470–1484
- 王岳军, 廖超林, 范蔚茗, 彭头. 2004. 赣中地区早中生代 OIB 碱性玄武岩的厘定及构造意义. *地球化学*, 33(2): 109–117
- 吴福元, 刘小驰, 纪伟强, 王佳敏, 杨雷. 2017. 高分异花岗岩的识别与研究. *中国科学(地球科学)*, 47(7): 745–765
- 肖娥, 邱检生, 徐夕生, 蒋少涌, 胡建. 2007. 浙江瑶坑碱性花岗岩体的年代学、地球化学及其成因与构造指示意义. *岩石学报*, 23(6): 1431–1440
- 谢昕, 徐夕生, 蒋少涌, 张明, 邱检生. 2005. 中国东南部晚中生代大规模岩浆作用序幕: J 早期玄武岩. *中国科学(D 辑)*, 35(7): 587–605
- 邢光福, 卢清地, 陈荣, 张正义, 聂童春, 李龙明, 黄家龙, 林敏. 2008. 华南晚中生代构造体制转折结束时限研究——兼与华北燕山地区对比. *地质学报*, 82(4): 451–463
- 许美辉. 1993. 永定五湖早侏罗世火山喷发盆地基本特征. *福建地质*, 12(3): 202–209
- 余心起, 狄永军, 吴淦国, 张达, 郑勇, 代堰鎔. 2009. 粤北存在早侏罗世的岩浆活动——来自霞岗杂岩 SHRIMP 锆石 U-Pb 年代学的证据. *中国科学(D 辑)*, 39(6): 681–693
- 张岳桥, 徐先兵, 贾东, 舒良树. 2009. 华南早中生代从印支期碰撞构造体系向燕山期俯冲构造体系转换的形变记录. *地学前缘*, 16(1): 234–247
- 张振杰, 左仁广. 2015. 闽西南地区大地构造演化和矿床时空分布规律. *岩石学报*, 31(1): 217–229
- 赵振华, 包志伟, 张伯友. 1998. 湘南中生代玄武岩类地球化学特征. *中国科学(D 辑)*, 28(增 1): 7–14
- 周金城, 陈荣. 2001. 闽东南晚中生代壳幔作用地球化学. *地球化学*, 30(6): 547–558
- 周金城, 蒋少涌, 王孝磊, 杨竞红, 张孟群. 2005. 华南中侏罗世玄武岩的岩石地球化学研究——以福建藩坑玄武岩为例. *中国科学(D 辑)*, 35(10): 927–936